An Electromyogram-Driven Musculoskeletal Model of the Knee to Predict *in Vivo* Joint Contact Forces During Normal and Novel Gait Patterns

Kurt Manal[1]
e-mail: manal@udel.edu

Thomas S. Buchanan

Delaware Rehabilitation Institute,
Department of Mechanical Engineering,
University of Delaware,
Newark, DE 19716

Computational models that predict internal joint forces have the potential to enhance our understanding of normal and pathological movement. Validation studies of modeling results are necessary if such models are to be adopted by clinicians to complement patient treatment and rehabilitation. The purposes of this paper are: (1) to describe an electromyogram (EMG)-driven modeling approach to predict knee joint contact forces, and (2) to evaluate the accuracy of model predictions for two distinctly different gait patterns (normal walking and medial thrust gait) against known values for a patient with a force recording knee prosthesis. Blinded model predictions and revised model estimates for knee joint contact forces are reported for our entry in the 2012 Grand Challenge to predict in vivo knee loads. The EMG-driven model correctly predicted that medial compartment contact force for the medial thrust gait increased despite the decrease in knee adduction moment. Model accuracy was high: the difference in peak loading was less than 0.01 bodyweight (BW) with an $R^2 = 0.92$. The model also predicted lateral loading for the normal walking trial with good accuracy exhibiting a peak loading difference of 0.04 BW and an $R^2 = 0.44$. Overall, the EMG-driven model captured the general shape and timing of the contact force profiles and with accurate input data the model estimated joint contact forces with sufficient accuracy to enhance the interpretation of joint loading beyond what is possible from data obtained from standard motion capture studies.
[DOI: 10.1115/1.4023457]

Keywords: joint contact, medial, lateral, modeling, inverse dynamics

Introduction

The medial compartment of the knee is most commonly affected in those with osteoarthritis (OA). Mechanical factors are believed to contribute to the genesis and progression of knee OA [1,2] and therefore methods which can predict changes in joint loading and how these forces are distributed between the medial and lateral compartments of the knee are of great interest to clinicians and researchers. It is not possible to measure joint forces *in vivo* except for a select few individuals who have undergone total knee arthroplasty with an instrumented prosthesis. In lieu of direct recordings, computational models have been used to predict joint loading during a variety of isometric and dynamic tasks [3–7].

The electromyogram (EMG) is a recording of the neuromuscular signal associated with muscle contraction. Muscle forces are the primary contributors to knee joint loading [7,8] and consequently how individuals activate their muscles has a direct impact on the pattern and magnitude of knee compressive forces. Patient populations including individuals with knee OA and those with anterior cruciate ligament (ACL) deficiency often use muscular coactivation to stabilize the knee [9–11] and in doing so exhibit altered loading [12,13]. For this reason, and because no two individuals activate their muscles exactly the same way, our approach has been to measure subject specific neuromuscular activation patterns and to use these as inputs when predicting muscle forces. We have used an EMG-driven musculoskeletal model of the knee to predict muscle and joint contact forces for healthy individuals [14,15], patients with ACL deficiency [13,16], OA [12], and following stroke [17].

Computational models, including our EMG-driven model, can lend insight into the mechanical environment of the knee and other structures. Despite this potential, many clinicians remain skeptical of modeling results in part due to poor communication between the research and clinical communities. It is imperative that methodological details be presented in a clear and concise manner so that one can appreciate the inherent assumptions and limitations of a given model. Furthermore, and perhaps more importantly, validation studies are generally lacking, making it difficult to critically evaluate the accuracy of a model, especially if model results are to be used to assist with patient planning and rehabilitation. It is exactly these reasons which motivated us to participate in the 2012 Grand Challenge to Predict *in vivo* Knee Forces. Newly added to this year's challenge was the opportunity to submit revised contact force estimates *after* original blinded predictions were submitted. Participants were provided the implant measured contact forces and these were used to guide adjustments to the model and/or model inputs.

The purposes of this paper are: (1) to describe our EMG-driven modeling approach to predict knee joint contact forces, and (2) to evaluate the accuracy of model predictions for two distinctly different gait patterns against known values for a patient with a force recording knee prosthesis. The data set is unique as it was obtained from an active female subject with an instrumented knee prosthesis allowing medial and lateral compartment forces to be resolved during dynamic activities. Forces measured by the prosthesis allowed us to compare our model estimates of medial and

[1]Corresponding author.

Contributed by the Bioengineering Division of ASME for publication in the JOURNAL OF BIOMECHANICAL ENGINEERING. Manuscript received October 19, 2012; final manuscript received January 16, 2013; accepted manuscript posted January 18, 2013; published online February 7, 2013. Editor: Beth Winkelstein.

lateral loading to known values experienced by the subject during normal and medial thrust gait. The strengths and weaknesses of our approach will be discussed and blinded force predictions and revised contact force estimates will be presented.

Methods

A description of the data collection and instrumentation, and a repository of the complete data set, can be found at https://simtk.org/home/kneeloads. The test subject was an active middle-age female (78.4 kg, 167 cm) with an instrumented left knee prosthesis. She completed a multitude of gait, strength, and functional trials all of which were available for download. The EMG-driven model we used to predict medial and lateral contact forces for two distinct walking patterns (normal walk and medial thrust gait) has been described in detail elsewhere [18] and thus only a brief summary of the key steps will be presented.

Step 1: Scale Subject Model. Bones and muscle attachment points for a nominal SIMM (software for interactive musculoskeletal modeling) musculoskeletal model of the left leg and pelvis were scaled to match the anthropometrics of the test subject determined from retroreflective markers placed over anatomical sites on the subject's pelvis, lower limb, and foot. These data were collected during a standing reference trial. Markers over the anterior superior iliac spines were used to adjust the width of the nominal SIMM male pelvis to match the pelvic width of the female test subject. The model included 12 muscles: sartorious, semimembranosus, semitendinosus, biceps femoris (long and short), tensor fascia latae, gastrocnemii (medial and lateral), rectus femoris, and three vasti (medial, lateral, and intermedius). The nominal SIMM model developed by Delp [19] was modified to include knee varus and valgus about contact points in the medial and lateral compartments, respectively (see step 3).

Step 2: EMG Processing. Recorded EMGs for the normal and medial thrust gait trials were high-pass filtered (fourth order Butterworth, cutoff 30 Hz), rectified, and subsequently low-pass filtered (cutoff 4 Hz) to create a linear envelope for each muscle. The linear envelopes were normalized to peak values obtained from a series of isometric and dynamic maximum effort trials that were collected for normalization purposes. The linear envelope for each muscle ranged between 0 and 1.0 [corresponding to $e(t)$ in Fig. 1]. EMG for the vastus intermedius was set equal to the average of the signals for the medial and lateral vasti. EMG for the semimembranosus and short head of biceps femoris were set equivalent to linear envelopes for the semitendinosus and long head of the biceps femoris, respectively. The reader is referred to Buchanan et al. [18] for details relating the coefficients which transform normalized EMG for each muscle $e(t)$ into muscle activation $a(t)$ for use with the musculoskeletal model.

Step 3: Inverse Dynamics. Marker trajectories and ground reaction force data were imported into Visual3D software to compute joint kinematics and moments. The marker trajectories were low-pass filtered using a zero-lag, fourth order Butterworth with a cut-off frequency of 6 Hz; ground reaction force data were low-pass filtered at 50 Hz. The markers were used to construct segment coordinate systems and define geometries for the left foot, leg, and the pelvis. An important consideration when defining the Visual3D model was to ensure the segment axes and locations of the joint centers were coincident with the subject scaled SIMM model described in step 1. The left leg and pelvis had a total of nine rotational degrees of freedom; three each for the left ankle, knee, and hip. Ankle dorsi/plantar flexion, knee flexion and adduction, and hip flexion angles specific to each gait trial were used as generalized coordinates with the subject scaled SIMM model to compute musculotendon lengths and sagittal plane moment arms. Segmental kinematics and ground reaction forces were combined to compute the net knee extensor moment which was used for model tuning outlined in step 5.

Two additional Visual3D and SIMM models were constructed; one each defining the medial and lateral compartments of the knee. The center of each compartment was fixed at $\pm 25\%$ of the tibial plateau width relative to the midpoint between the markers positioned over the femoral condyles. These points were assumed to represent the medial and lateral points of contact between the femur and tibial plateau and were specified in the SIMM and Visual3D models. Muscle moment arms in the frontal plane about the medial and lateral contact points were computed using SIMM. Knee adduction moments about the medial and lateral contact points were calculated using Visual3D. These data in addition to muscle forces described in step 4 were then applied to a frontal plane moment balancing algorithm in step 6 to distribute the total joint contact to the medial and lateral compartments.

Step 4: Muscle Force Model. The force generating element in our EMG-driven model is a Hill-type muscle fiber in series with an elastic tendon. The muscle fiber has a contractile component in parallel with an elastic element as seen in Fig. 2. Individual muscle fibers comprising a muscle-tendon unit are assumed to be identical in structure as other fibers and thus the force a muscle generates is a scaled-up version of a single muscle fiber (Fig. 2). The state variables in our implementation of the Hill model included muscle activation and fiber length.

The force generated by a muscle F^m is a function of the muscle's activation (a), fiber length (l^m), velocity (v^m), and pennation angle ($\varnothing$). All of these variables change as a function of time (t). Muscle force is also dependent on musculoskeletal parameters that are assumed not to change with time: optimal fiber length (l_o^m), tendon slack length (l_s^t), and maximum isometric muscle force (F_o^m),

$$F^m(t) = f\left(a(t), l^m(t), v^m(t), \varnothing(t), l_o^m, l_s^t, F_o^m\right) \tag{1}$$

Time invariant parameters are initially set to average values obtained from the literature [20] and time varying variables are computed dependent on the joint kinematics the relevant muscle spans. Coefficients which transform normalized EMG $e(t)$ to muscle activation $a(t)$ are initialized with zero electromechanical delay and a linear relationship (see Buchanan et al. [18]). That is,

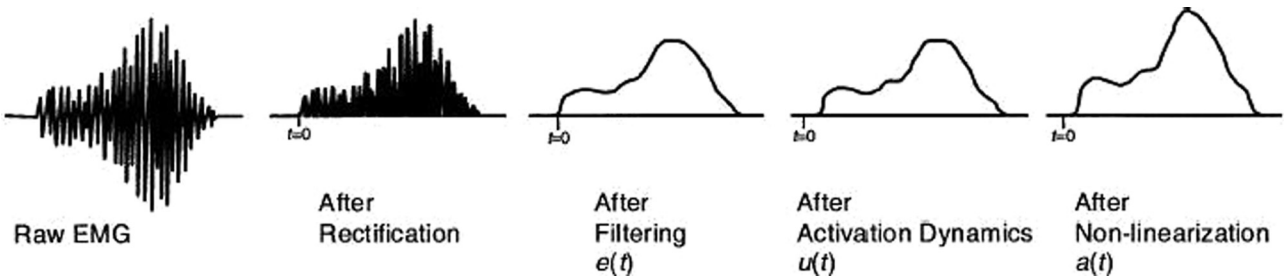

Fig. 1 Transformation of raw EMG to muscle activation $a(t)$ as an input to the EMG-driven model (from [18])

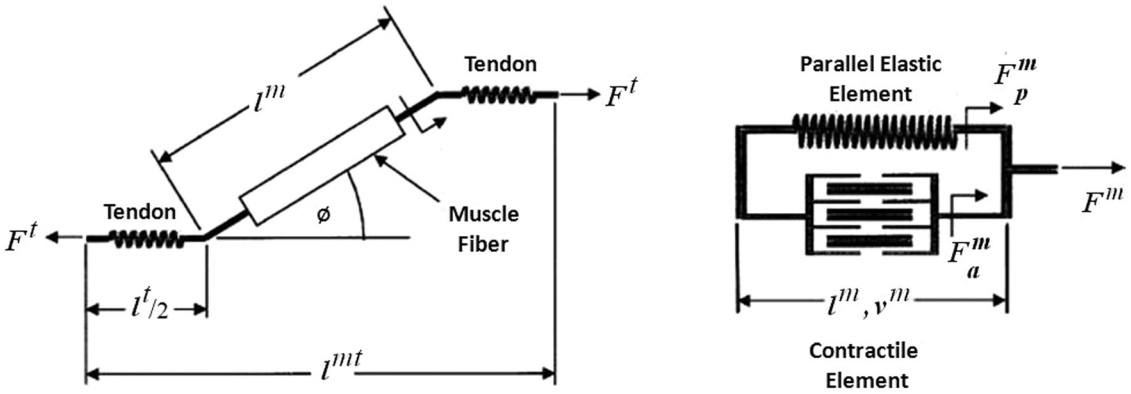

Fig. 2 Schematic of a Hill-type muscle fiber. The musculotendon unit (shown on the left) has a muscle fiber in series with tendon. The musculotendon length l^{mt} is the sum of the fiber length l^m, adjusted for pennation angle Ø, and the tendon length l^t. The muscle fiber shown on the right is comprised of an active contractile element in parallel with a passive elastic element. F^m_a is the force developed by active mechanisms (i.e., length-tension and force-velocity relationships). F^m_p represents the passive force contribution when the muscle fiber is at a length beyond optimal (i.e., passive portion of the length-tension curve). The active and passive forces sum to yield the fiber force F^m, and when adjusted for pennation angle is equivalent to the force acting through the tendon F^t.

the coefficients are initialized such that muscle activation is equivalent to normalized EMG. The tendon excursion method [21] is used to compute sagittal plane moment arms which are then multiplied by the corresponding muscle forces and summed to yield a model-computed net extensor moment. The modeled moment is of course sensitive to the initial values chosen for muscle parameters and activation coefficients and these values are adjusted as described in step 5.

Step 5: Model Tuning. The purpose of model tuning is to identify a set of muscle parameters and coefficients which generate muscle forces that when multiplied by their respective moment arms sum to yield a model predicted moment that is in close agreement with the moment computed from inverse dynamics. Considering the model is initialized with average values from the literature, it is not surprising it does not closely match at the outset. Note that model tuning does not manipulate the modeled-moment curve directly, but rather it adjusts the muscle forces by changing parameters and coefficients such that the squared difference between the model predicted moment and the moment from inverse dynamics is minimized. Initial values for the muscle parameters and activation coefficients are adjusted iteratively using a simulated annealing algorithm [22]. Muscle parameters are allowed to vary within ±2 SDs of values reported in the literature and the value for electromechanical delay is constrained between 0 and 70 ms. A schematic of the tuning process is shown in Fig. 3. The normal walk and medial thrust gait were tuned at the same time resulting in one set of muscle parameters. Tuning the EMG-driven model to the knee extensor moment does not ensure a unique distribution of muscle forces. Penalty functions were applied to eliminate unrealistic solutions in which a muscle generates large passive forces or does not generate force even though the muscle is actively contracting as indicated when $e(t)$ is greater than 0. Constraints on optimal fiber length and tendon slack length are enforced by penalty functions to maintain normalized fiber length between 0.6 and 1.2 and to prevent negative tendon strains.

Step 6: Medial and Lateral Contact Forces. Knee adduction moments and moment arms about the medial and lateral contact points defined in step 3 and muscle forces from step 5 were input to a frontal plane moment balancing algorithm to determine the unknown medial and lateral contact forces. The method can be summarized as follows with more specific details provided by Winby and colleagues [23]. The external knee adduction moment about the lateral contact point computed from inverse dynamics must be balanced internally by muscle forces relative to the lateral point of contact and an unknown medial contact force acting at one half the width of the tibial plateau. The distance between the contact force and the opposite point of contact will be referred to as the lever arm (labeled "d" in Fig. 4). This process is repeated at every time step during the gait cycle. Tensile forces from collateral ligaments and the joint capsule were not required to balance the moment in the frontal plane since both compartments were assumed to remain in compression throughout stance. This was subsequently verified using the knee implant data. Moments in the transverse plane were not considered based on the assumption that only forces perpendicular to the tibial plateau or those which generate an adduction moment about the knee contribute to joint compressive force aligned with the long axis of the tibia. The same approach was used to determine lateral contact forces.

Results

The EMG-driven model captured the general shape and timing for all contact force patterns, most notably for the medial thrust gait (Fig. 5). These data represent our blinded model predictions of forces recorded by the instrumented knee implant. There are several interesting observations that warrant attention. First, the model predicted medial contact force for the medial thrust gait matched extremely well ($R^2 = 0.92$) with negligible differences in peak loading (<0.01 BW). Peak force for the lateral compartment was overestimated by approximately 0.6 BW, and the model captured the shape and timing of the contact force profile. An opposite trend was noted for the normal walking trial. That is, the model successfully predicted peak lateral contact and there was a strong positive relationship ($R^2 = 0.44$) between the predicted and measured data. Peak medial force for the normal walking trial was underestimated by approximately one half bodyweight and once again the model captured the general shape and timing of the loading profile. Descriptive statistics for the blinded model predictions are reported in Table 1. Model predictions were best for the medial compartment during medial thrust gait and for the lateral compartment during normal gait.

Revised contact force estimates for the two gait patters are shown in Fig. 6. Note how we use the term estimates in place of predictions as these data reflect changes to the model that were made in part based on knowledge of the forces recorded by the implant. Revisions to the model included: (1) use of an accurate measure of tibial plateau width, (2) allowing the medial and lateral contact points to vary slightly from previously defined locations, and (3) separate tunings for normal and medial thrust gait

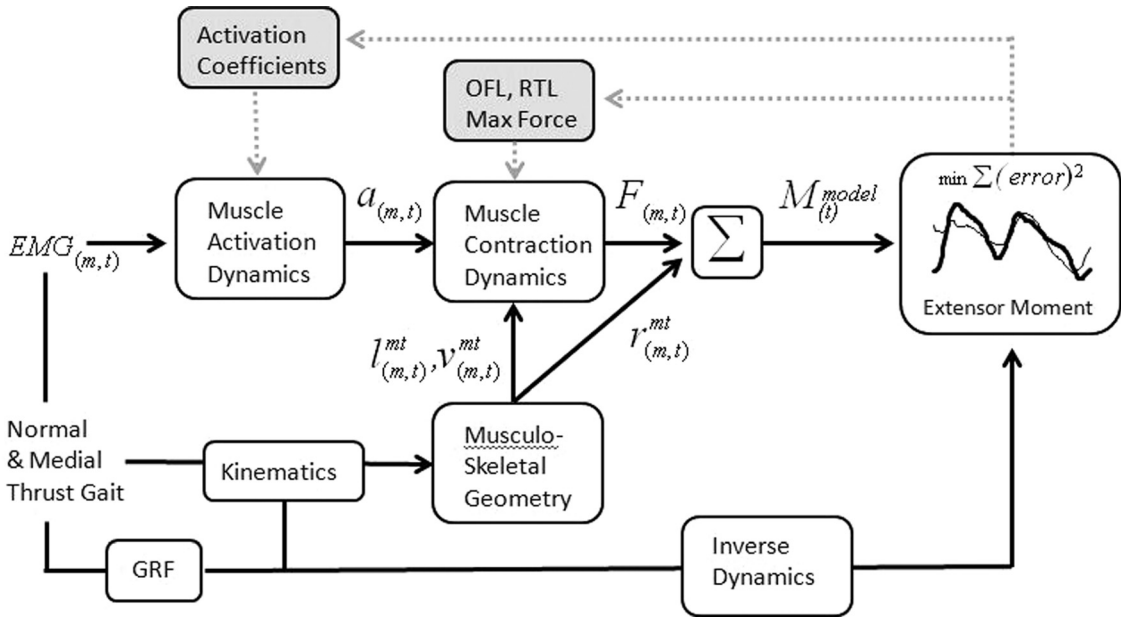

Fig. 3 EMG for muscle *m* at time *t* was transformed into muscle activation *a* to activate a Hill-type muscle model (muscle contraction dynamics). The force *F* for each muscle was then multiplied by its sagittal plane moment arm *r* according to the musculoskeletal geometry which is dependent on the joint kinematics for the particular trial. Individual muscle moments are then summed at each point in time to obtain a model estimated sagittal plane knee moment. The knee moment was also calculated using inverse dynamics from video-based motion data and ground reaction forces. EMG-driven model parameters including activation coefficients, optimal fiber length (OFL), resting tendon length (RTL), and the maximum isometric force for each muscle were adjusted iteratively to minimize the sum-squared difference between the model estimated moment and the moment computed from inverse dynamics. The process of optimally adjusting model parameters is depicted by the gray shaded boxes and dashed arrows.

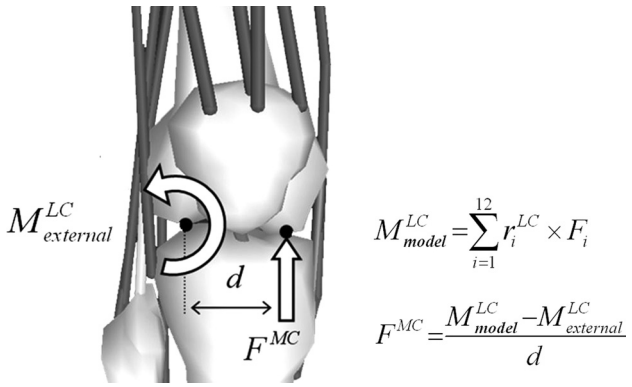

Fig. 4 Schematic of the moment balancing algorithm to compute medial contact force (F^{MC}). The external adduction moment about the lateral condyle $M^{LC}_{external}$ must be balanced by a moment generated by muscles M^{LC}_{model} and an unknown contact force F^{MC} acting at distance *d* equal to one half the width of the tibial plateau. r_i^{LC} is the moment arm for muscle *i* relative to the lateral condyle and F_i is the force generated by the muscle.

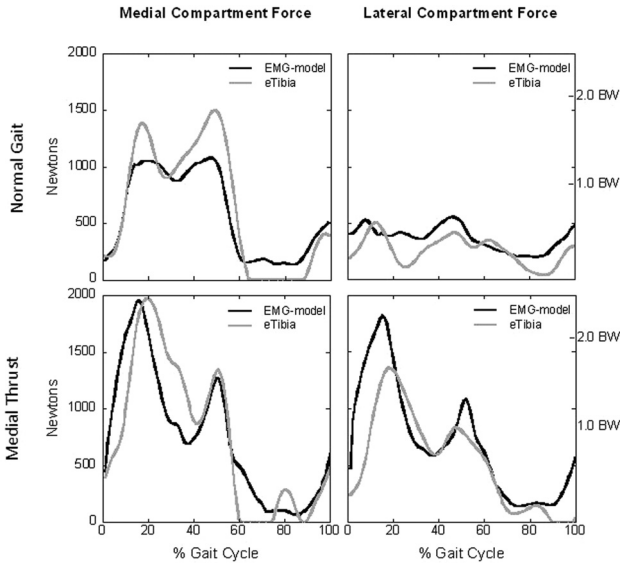

Fig. 5 The dark lines represent the EMG-driven model's prediction of joint contact force and the gray lines are the forces measured by the instrumented knee implant (eTibia). The model captured the general shape and timing of the contact force profiles with good predictions of medial contact for the medial thrust gait and lateral contact for normal walking. The largest difference between the model predicted and measured force was for the lateral compartment during medial thrust gait.

were conducted. How these modifications were implemented will be addressed in the Discussion. Two improvements are immediately apparent. First, the model-estimated medial contact force for the normal gait pattern is now in close agreement with the force measured by the implant. Second, the difference between peak lateral contact for the medial thrust gait dropped from 0.59 to 0.13 BW and agrees much more closely with the force recorded by the implant. This was the largest difference in peak loading with all other differences less than 0.05 BW. Descriptive statistics for the revised contact force estimates are included in Table 1.

Discussion

Computational models have the potential to lend insight into normal and pathological movement and complement interpretations based on findings obtained from standard motion capture studies. This has motivated us to apply our EMG-driven model to

Table 1 Descriptive statistics for the original model predictions and revised estimates. Peak diff (BW) is the difference in peak contact force between the model and the implant reported in bodyweights. Rmse = root mean square error over the entire stride.

		Normal gait		Medial thrust	
	Prediction	Medial	Lateral	Medial	Lateral
Peak diff (BW)	Original	−0.55	+0.04	< 0.01	+0.59
	Revised	+0.03	< 0.01	+0.05	+0.13
R^2	Original	0.92	0.44	0.75	0.66
	Revised	0.95	0.03	0.84	0.55
rmse (BW)	Original	0.28	0.18	0.41	0.42
	Revised	0.16	0.22	0.34	0.37

healthy patient populations to understand muscle and joint contact forces during activities of daily living and how these forces change in response to therapy and rehabilitation. Out first goal for this paper was to describe our modeling framework to predict medial and lateral knee joint contact forces. The description was intended as an overview with sufficient detail to understand the general modeling flow and to appreciate why specific modifications to the model were considered when revising our estimates of joint contact force. The reader is directed to Buchanan et al. [18] for more details and discussion of our implementation of the EMG-driven musculoskeletal model. The second goal of this work was to compare our predictions of joint contact forces to known values recorded for a patient with an instrumented knee prosthesis, using the data supplied by the Grand Challenge. Studies of this kind are helpful for the clinical community to recognize the potential of such models to assist with patient treatment. Furthermore, it is important to evaluate the efficacy of a model not only under idealized conditions such as normal walking, but also when the model is applied to novel gait patterns. Model predictions were made for two distinctly different walking styles; normal and medial thrust gait. Medial thrust gait was developed to reduce the peak knee adduction moment. The adduction moment is often used as a surrogate measure of medial compartment loading and a decrease in adduction moment is assumed to correspond to a decrease in medial joint contact. Walter and colleagues however have shown that this is not always the case. Using instrumented knee data from another patient they showed that a decrease in knee adduction moment does not guarantee decreased medial contact force during gait [24].

Examining Fig. 5 and Table 1 it is immediately apparent that the EMG-driven model did extremely well predicting medial contact force for the medial thrust gait. This novel gait pattern was designed to reduce peak knee adduction moment and ostensibly peak medial contact. Interestingly, our EMG-driven model predicted an increase in medial contact force compared to normal gait, and this was at first disconcerting considering the adduction moment for medial thrust gait (data not shown) was smaller than normal (27 versus 15 Nm). Based on the moment data alone one might have inferred a decrease in medial contact force. However, this was not the case and our prediction of increased loading was

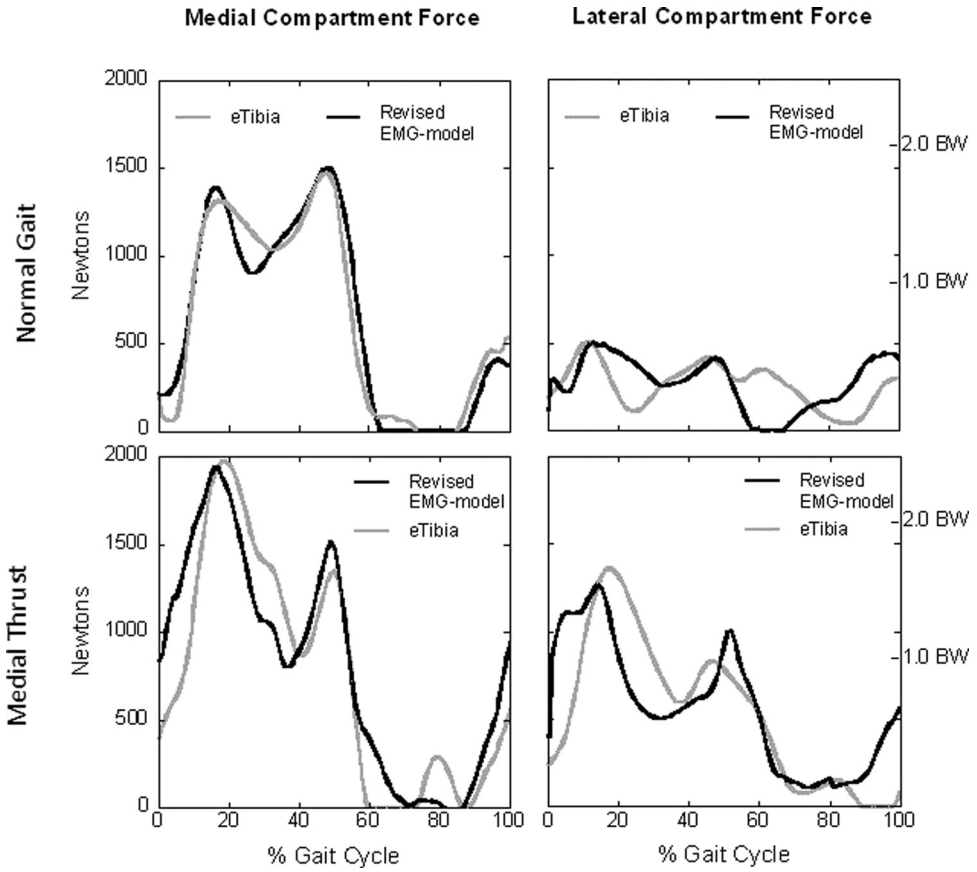

Fig. 6 The dark lines represent the revised force estimates for the EMG-driven model and the gray lines are the forces measured by the instrument ted knee implant (eTibia). The revised model captured the general shape and timing of the contact force profiles with good agreement in peak values. The largest difference between the model predicted and measured force was 0.13 BW for the lateral compartment during medial thrust gait. All other difference in peak values were less than 0.05 BW.

confirmed by data from the instrumented knee implant (Fig. 5). Medial thrust gait for this patient increased medial loading by approximately 0.6 BW even though adduction moment was greatly reduced. Our model predicted exactly this increase and the difference between peak medial loading and the force measured by the instrumented knee was negligible (<0.01 BW). Also note the model successfully predicted a second peak medial force and there was excellent temporal alignment between the predicted force and medial contact measured by the instrumented knee.

Model predictions for lateral contact force are shown in Fig. 5. Although the model did capture the general shape and timing of the lateral contact profile, peak force was overestimated by 0.59 BW. This difference is significant considering the peak force recorded by the knee prosthesis was 1.73 BW. It is interesting to note exactly when the opposite trend was observed when predicting medial and lateral forces for the normal walking trial. That is, the EMG-driven model underestimated medial loading and predicted peak forces for the lateral compartment quite well. Peak loading for the medial compartment during normal gait was approximately 390 N less than recorded by the implant. The peak difference for the lateral compartment was negligible (+0.04 BW) and qualitatively the shape of the curve followed the pattern for the measured forces with an R^2 of 0.44, corresponding to a strong positive correlation of 0.66 (see Table 1).

While we are pleased with the results, there are several sources of error that should be addressed so that the model can be evaluated and future improvements can be made. There are many small sources of noise and/or error that influence the calculation of joint moments including: marker measurement error, soft tissue movement error, EMG quality, incorrectly aligned joint and segmental axes, and small errors in the center of pressure. Individual muscle forces contributing to the net extensor moment were obtained from the model tuning process and thus inaccuracies when calculating joint moments will map into errors in muscle force and subsequent predictions of joint contact. These errors can be difficult to trace, especially considering the data were not collected in our laboratory. Larger sources of error are more concretely identified and were the focus of our revised model estimates. Furthermore, a decision was made regarding which parameters to adjust in the optimization and we decided only to consider model inputs that could be determined from patient and experimental data without explicit information from the knee prosthesis. As such our revised estimates were not merely a curve fitting exercise. The three modifications incorporated in our revised estimates were: (1) more accurate measure of tibial plateau width, (2) allowing the medial and lateral contact points to vary slightly relative to the originally defined locations on the tibial plateau, and (3) separate tunings for the normal and medial thrust gait. We will focus the following discussion on how these three factors improved our model estimates without describing exactly why predictions that were good to begin with remained relatively unchanged.

The first modification and the most important was using an accurate measure of the tibial plateau width. Our initial estimate was too large and this had a direct effect on the location of the medial and lateral contact points. As a result the muscle moment arms about the medial and lateral contact points and the lever arm for the medial and lateral contact forces were too large. The actual implant width of 0.074 m was obtained from the implant geometry and this was approximately 50% smaller than the width we estimated from the motion capture data. The data provided by the Grand Challenge did not include all of the measurements that are usually recorded in our lab which are designed to minimize these errors, so we had to improvise. By not accounting for skin and adipose tissue thickness and other unknowns including marker diameter and the manner in which the markers were attached (e.g., adhered to the skin directly or mounted on small posts), we were required to estimate some values in the absence of actual data. When possible we measure the width of the tibial plateau from long cassette X-rays, but there are times when estimates are based on motion capture data from markers over the distal femur. When doing so we account for offsets associated with the markers and also include an estimate of subcutaneous fat and other tissues based on skin-fold caliper measurements. Additionally, our estimate for the plateau width was based on markers positioned over the femoral condyles. The width of the distal femur is approximately 5%–10% greater than the width of the tibial plateau and this too contributed to our using too large a value. When the Visual3D and SIMM models were modified to account for the actual width of the tibial plateau, several noteworthy and predictable changes resulted. Obtaining an accurate estimate of tibial plateau width is important when computing medial and lateral contact forces using methods outlined in this study.

The second modification was to allow the medial and lateral contact points to vary slightly relative to the originally defined locations on the tibial plateau. It was observed that the adduction moment about the medial and lateral contact points for the two gait patterns all decreased in magnitude. The largest change was a 55% decrease in adduction moment for the medial compartment when walking with a medial thrust gait. The smaller moment about the medial contact point required less lateral contact force to balance the moment even though the lever arm was shorter. This was possible because the decrease in the moment about the medial contact point was greater than the change in the lever arm. Less important, but beneficial nonetheless, was that we shifted the lateral contact point laterally by approximately 3 mm corresponding to 4% of the tibial plateau width. The percent change was determined iteratively until a qualitative fit of the model better matched the force recorded by the implant. The revised and improved estimates are shown in Fig. 6 and described in Table 1.

The third modification was that separate parameter adjustments were made for the normal and medial thrust gait. After viewing the actual results from the instrumented knee we observed that the peak loading for the medial and lateral compartments during medial thrust gait occurred during weight acceptance in early stance. The quadriceps contract eccentrically during this time creating a net extensor moment that controls knee flexion during weight acceptance. The peak extensor moment for the medial thrust gait was approximately 110 Nm while the peak moment for normal walking was only 20 Nm. The objective of the model tuning process described in step 5 was to converge on a set of muscle parameters and coefficients which minimized the difference between the model-computed knee extensor moments and the moments computed from inverse dynamics. The medial thrust and normal walking trials were tuned at the same time and although we did attempt to weight the objective function for large differences in knee extensor moment magnitude, the simulated annealing optimization was biased towards fitting the larger moment associated with the medial thrust gait. To improve our revised estimates we tuned the trials separately. This had little effect on muscle forces for the medial thrust gait because of the original bias when the trials were tuned simultaneously. However, this resulted in two sets of muscle parameters and activation coefficients. This is less than ideal and clearly nonphysiologic. Nonetheless a goal of the revised estimates was to identify aspects of our model that could be adjusted to promote better agreement with the forces measured by the implant. We observed that the reason separate tunings benefited the normal walk trial was related to the large differences in magnitude between the medial thrust and normal walking gaits. From this we learned that combined tunings of widely disparate moment curves can bias the selection of muscle parameters and activation coefficients favoring the trial with the larger moment. We are evaluating different weighting functions to more effectively tune widely different joint moments at the same time to obtain an optimal set of muscle parameters and activation coefficients. This is important towards our long-term goal of developing high-quality patient specific models by measuring as many parameters as possible and allowing the optimizer to select those that cannot be measured.

Computational models that predict internal forces have the potential to enhance our understanding of normal and pathological

movement. A perfect example of this was seen when applying our model to the medial thrust gait. This walking pattern was designed to reduce the knee adduction moment and it did so effectively. The adduction moment dropped significantly and from this one might have inferred that medial compartment loading also decreased. However, our model correctly predicted exactly the opposite and this was validated by data from the instrumented knee. This demonstrates the value of our modeling approach. It is our sincere hope that clinicians will recognize the insight computational models can provide. For patient populations that use altered neuromuscular activation patterns, we suggest that models account for those changes using EMGs or other measures of neural command.

Acknowledgment

This work supported, in part, by NIH R01-AR046386 and R01-AR048212.

References

[1] Andriacchi, T. P., and Mundermann, A., 2006, "The Role of Ambulatory Mechanics in the Initiation and Progression of Knee Osteoarthritis," Curr. Opin. Rheumatol., **18**, pp. 514–518.
[2] Sharma, L., Hurwitz, D. E., Thonar, E. J., Sum, J. A., Lenz, M. E., Dunlop, D. D., Schnitzer, T. J., Kirwan-Mellis, G., and Andriacchi, T. P., 1998, "Knee Adduction Moment, Serum Hyaluronan Level, and Disease Severity in Medial Tibiofemoral Osteoarthritis," Arthritis Rheum., **41**, pp. 1233–1240.
[3] Lloyd, D. G., and Buchanan, T. S., 1996, "A Model of Load Sharing Between Muscles and Soft Tissues at the Human Knee During Static Tasks," ASME J. Biomech. Eng., **118**, pp. 367–376.
[4] Buchanan, T. S., Lloyd, D. G., Manal, K., and Besier, T. F., 2005, "Estimation of Muscle Forces and Joint Moments Using a Forward-Inverse Dynamics Model," Med. Sci. Sports Exercise, **37**, pp. 1911–1916.
[5] Manal, K., Gravare-Silbernagel, K., and Buchanan, T. S., 2011, "A Real-Time EMG-Driven Musculoskeletal Model of the Ankle," Multibody Syst. Dyn., **28**, pp. 169–180.
[6] Xiao, M., and Higginson, J., 2010, "Sensitivity of Estimated Muscle Force in Forward Simulation of Normal Walking," J. Appl. Biomech., **2**, pp. 142–149.
[7] Sasaki, K., and Neptune, R. R., 2010, "Individual Muscle Contributions to the Axial Knee Joint Contact Force During Normal Walking," J. Biomech., **43**, pp. 2780–2784.
[8] Herzog, W., Longino, D., and Clark, A., 2003, "The Role of Muscles in Joint Adaptation and Degeneration," Langenbecks Arch. Surg., **288**, pp. 305–315.
[9] Rudolph, K. S., Axe, M. J., Buchanan, T. S., Scholz, J. P., and Snyder-Mackler, L., 2001, "Dynamic Stability in the Anterior Cruciate Ligament Deficient Knee," Knee Surg. Sport Tr. A., **9**, pp. 62–71.
[10] Chmielewski, T. L., Hurd, W. J., Rudolph, K. S., Axe, M. J., and Snyder-Mackler, L., 2005, "Perturbation Training Improves Knee Kinematics and Reduces Muscle Co-Contraction After Complete Unilateral Anterior Cruciate Ligament Rupture," Phys. Ther., **85**, pp. 750–754.
[11] Hubley-Kozey, C., Deluzio, K., and Dunbar, M., 2008, "Muscle Co-activation Patterns During Walking in Those With Severe Knee Osteoarthritis," Clin. Biomech., **23**, pp. 71–80.
[12] Kumar, D., Rudolph, K. S., and Manal, K., 2011, "EMG-Driven Modeling Approach to Muscle Force and Joint Load Estimations: Case Study in Knee Osteoarthritis," J. Orthop. Res., **30**, pp. 377–383.
[13] Gardinier, E., Manal, K., Buchanan, T. S., and Snyder-Mackler, L., 2013, "Altered Loading in the Injured Knee after ACL Rupture," J Orthop Res. **31**(3), pp. 458–464.
[14] Manal, K., Kumar, D., Rudolph, K. S., and Buchanan, T. S., 2010, "Joint Loading During Gait in Those With Medial Compartment Knee Osteoarthritis and Healthy Controls," Proc. World Congress on Biomechanics, VI, CD.
[15] Manal, K., Kumar, D., Buchanan, T. S., and Rudolph, K. S., 2010, "Joint Contact Force Comparisons Between Healthy Subjects and Those With Medial Compartment Knee Osteoarthritis," Proc. Am. Soc. Biomech. **34**, CD.
[16] Gardinier, E. S., Manal, K., Buchanan, T. S., and Snyder-Mackler, L., 2012, "Gait and Neuromuscular Asymmetries After Acute Anterior Cruciate Ligament Rupture," Med. Sci. Sports Exerc., **44**, pp. 1490–1496.
[17] Shao, Q., Bassett, D. N., Manal, K., and Buchanan, T. S., 2009, "An EMG-Driven Model to Estimate Muscle Forces and Joint Moments in Stroke Patients," Comput. Biol. Med., **39**, pp. 1083–1088.
[18] Buchanan, T. S., Lloyd, D. G., Manal, K., and Besier, T. F., 2004, "Neuromusculoskeletal Modeling: Estimation of Muscle Forces and Joint Moments and Movements From Measurements of Neural Command," J. Appl. Biomech., **20**, pp. 367–395.
[19] Delp, S. L., Loan, J. P., Hoy, M. G., Zajac, F. E., Topp, E. L., and Rosen, J. M., 1990, "An Interactive Graphics-Based Model of the Lower Extremity to Study Orthopaedic Surgical Procedures," IEEE Trans. Biomed. Eng., **37**, pp. 757–767.
[20] Yamaguchi, G. T., Sawa, A. G. U., Moran, D. W., Fessler, M. J., and Winters, J. M., 1990, "A Survey of Human Musculotendon Actuator Parameters," *Multiple Muscle Systems, Biomechanics and Movement Organization*, J. M. Winters and S.L-Y. Woo, eds., Springer, New York, pp. 717–774.
[21] An, K. N., Takahashi, K., Harrigan, T. P., and Chao, E. Y., 1984, "Determination of Muscle Orientations and Moment Arms," ASME J. Biomech. Eng., **106**, pp. 280–282.
[22] Goffe, W. L., Ferrier, G. D., and Rogers, J., 1994, "Global Optimization of Statistical Functions With Simulated Annealing," J. Econometrics, **60**, pp. 65–100.
[23] Winby, C. R., Lloyd, D. G., Besier, T. F., and Kirk, T. B., 2009, "Muscle and External Load Contribution to Knee Joint Contact Loads During Normal Gait," J. Biomech., **42**, pp. 2294–2300.
[24] Walter, J. P., D'Lima, D. D., Colwell, C. W., and Fregly, B. J., 2010, "Decreased Knee Adduction Moment Does Not Guarantee Decreased Medial Contact Force During Gait," J. Orthop. Res., **28**, pp. 1348–1354.